Quantifying Steric Effects of α-Diimine Ligands. Oxidative Addition of MeI to Rhodium(I) and Migratory Insertion in Rhodium(III) Complexes

Luca Gonsalvi,[†,‡] Joseph A. Gaunt,[†] Harry Adams,[†] Aurora Castro,[†] Glenn J. Sunley,*[,§] and Anthony Haynes*[,†]

Department of Chemistry, University of Sheffield, Sheffield, U.K. S3 7HF, and Hull Research and Technology Centre, BP Chemicals Ltd., Saltend, Hull, U.K. HU12 8DS

Received September 17, 2002

The series of Rh(I) complexes [Rh(CO)(diimine)I] have been prepared (diimine = ArN=C(Me)C(Me)=NAr, Ar = 2-^{i}PrC$_6$H$_4$ (**1a**), 2,4,6-Me$_3$C$_6$H$_2$ (**1b**), 2,6-^{i}Pr$_2$C$_6$H$_3$ (**1c**); diimine = ArN=C(Me)-2-py, Ar = C$_6$H$_5$ (**1d**), 2-^{i}PrC$_6$H$_4$ (**1e**), 2,6-^{i}Pr$_2$C$_6$H$_3$ (**1f**); diimine = 2,2′-bipy (**1g**)). An X-ray crystal structure showed **1f** to have CO trans to the pyridyl nitrogen. Oxidative addition of MeI to **1a**,**d**,**e**,**g** gave the stable methyl complexes [Rh(CO)(diimine)I$_2$Me] (**2a**,**d**,**e**,**g**, respectively); an X-ray structure for **2a** showed a pseudo-octahedral geometry with methyl trans to iodide. In contrast, the reactions of **1b**,**c** with MeI gave the five-coordinate acetyl complexes [Rh(diimine)I$_2$(COMe)] (**3b**,**c**, respectively); an X-ray structure for **3c** displayed a distorted-square-pyramidal geometry. The methyl complex **2b** was detected as a reactive intermediate during the reaction of **1b**. The reaction of **1f** with MeI attained an equilibrium with the methyl and acetyl products **2f** and **3f**. The different outcomes result from diimine ligand steric effects, with bulky alkyl groups in the ortho positions of N-aryl groups favoring migratory CO insertion. Rearrangement from octahedral to square-pyramidal geometry relieves steric strain between axial ligands and ortho alkyl substituents on the diimine. Kinetic studies showed that the second-order rate constant (k_1) for MeI oxidative addition varied by a factor of $>10^3$, depending on the steric bulk of the diimine ligand. For the bipy complex **1g**, k_1 is the highest yet reported for a Rh(I) carbonyl complex (0.206 M^{-1} s^{-1}, CH_2Cl_2, 25 °C). Kinetic data are also reported for migratory CO insertion in **2b**,**f**. An X-ray structure of [Rh(CO)(ArN=C(Me)-2-py)I$_3$] (**4f**; Ar = 2,6-^{i}Pr$_2$C$_6$H$_3$), the product of oxidative addition of I$_2$ to **1f**, reveals distortion from ideal octahedral geometry caused by ortho ^{i}Pr groups on the diimine ligand.

Introduction

Recent advances in organometallic chemistry and homogeneous catalysis have emphasized the important role of ligand steric effects. In particular, it has been found that N-aryl ortho substituents in α-diimines (Ar$_2$DAB) and pyridyl diimines are key to the behavior of olefin polymerization catalysts based on group 8−10 metals.[1,2] Steric bulk inhibits associative chain transfer relative to propagation and so favors the production of high-molecular-weight polymers.[3] Steric effects also influence the behavior of complexes of the type [Pt(diimine)(L)R]$^+$ in C−H activation reactions[4] and in ion-pairing interactions.[5] In this paper we report the quantification of steric effects of α-diimine ligands on oxidative addition and migratory insertion in a model rhodium system.

We recently reported some dramatic ligand effects on the rate of migratory CO insertion in complexes of the type [Rh(CO)(L−L)I$_2$Me] (L−L = Ph$_2$PCH$_2$P(S)Ph$_2$ (dppms), Ph$_2$PCH$_2$CH$_2$PPh$_2$ (dppe)).[6] An X-ray crystal structure of the stable [Ir(CO)(dppms)I$_2$Me] showed the methyl ligand to be placed in a sterically congested region created by the ligand phenyl substituents. We proposed that this steric crowding contributed to the much faster migratory insertion in [Rh(CO)(dppms)-I$_2$Me] than in the dppe analogue. These findings led us to carry out further studies on the [Rh(CO)(L−L)I] + MeI system using bidentate ligands in which steric bulk could be easily controlled. The α-diimines used by Brookhart[2] and others[4,7−12] provided the ideal characteristics for this study.

* To whom correspondence should be addressed. E-mail (A.H.): a.haynes@sheffield.ac.uk.
† University of Sheffield.
‡ Current address: Institute for the Chemistry of Organometallic Compounds, National Research Council (ICCOM-CNR), Via J Nardi 39-41, 50132, Firenze, Italy.
§ BP Chemicals Ltd.

(1) Britovsek, G. J. P.; Gibson, V. C.; Wass, D. F. *Angew. Chem., Int. Ed. Engl.* **1999**, *38*, 428.
(2) Ittel, S. D.; Johnson, L. K.; Brookhart, M. *Chem. Rev.* **2000**, *100*, 1169.
(3) Tempel, D. J.; Johnson, L. K.; Huff, R. L.; White, P. S.; Brookhart, M. *J. Am. Chem. Soc.* **2000**, *122*, 6686.
(4) Zhong, H. A.; Labinger, J. A.; Bercaw, J. E. *J. Am. Chem. Soc.* **2002**, *124*, 1378. Johansson, L.; Ryan, O. B.; Rømming, C.; Tilset, M. *J. Am. Chem. Soc.* **2001**, *123*, 6579.
(5) Zuccaccia, C.; Macchioni, A. *Organometallics* **1999**, *18*, 4367.
(6) Gonsalvi, L.; Adams, H.; Sunley, G. J.; Ditzel, E.; Haynes, A. *J. Am. Chem. Soc.* **1999**, *121*, 11233. Gonsalvi, L.; Adams, H.; Sunley, G. J.; Ditzel, E.; Haynes, A. *J. Am. Chem. Soc.* **2002**, *124*, 13597.
(7) van Koten, G.; Vrieze, K. *Adv. Organomet. Chem.* **1982**, *21*, 151.

10.1021/om020777w CCC: $25.00
Publication on Web 01/25/2003

Scheme 1. Synthesis and Numbering Scheme for Complexes 1a−g

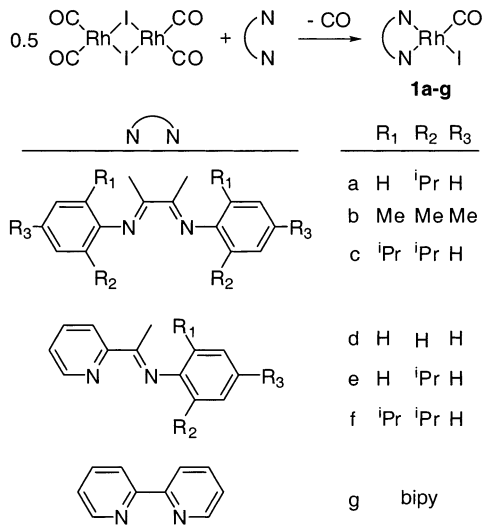

Results and Discussion

Synthesis and Characterization of Rh(I) Complexes. Symmetrical diimines and unsymmetrical pyridylimines were prepared by condensation of the appropriate amine and ketone. An X-ray crystal structure (Supporting Information) of ArN═C(Me)C(Me)═NAr (Ar = 2-^{i}PrC$_6$H$_4$) revealed an *E,s-trans-E* conformation for the free ligand, as reported for CyN═CHCH═NCy.[7,13] Complexation of the diimine ligands to Rh(I) was achieved by reaction with the dimer $[Rh(CO)_2I]_2$ (Scheme 1).[14] The products, [Rh(CO)(diimine)I][15] (**1a**−**f**), were isolated as strongly colored crystalline solids and fully characterized by spectroscopy, elemental analysis, and, in the case of **1f**, an X-ray crystal structure. The bipy complex **1g** has been reported previously.[16]

The infrared spectra of complexes **1a**−**c** displayed almost identical ν(CO) values, indicating that variation of the alkyl substituents on the N-aryl groups has little influence on the donor ability of the diimine ligand. Likewise, complexes **1d**−**f** have ν(CO) values which lie very close to each other but are ca. 5 cm^{-1} lower than those of **1a**−**c**, suggesting that the pyridyl nitrogen is a slightly better donor than the exocyclic imine. This is supported by the observation that ν(CO) for the bipy complex **1g** is ca. 10 cm^{-1} lower than for **1d**−**f**.

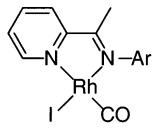

Figure 1. Stereochemistry of pyridylimine complexes **1d**−**f**.

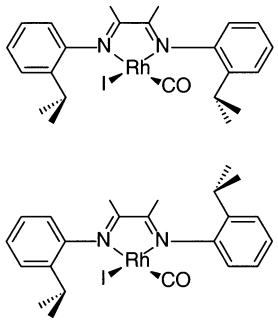

Figure 2. Conformers of complex **1a**.

^{1}H NMR spectroscopy indicated that each of the pyridylimine complexes **1d**−**f** is formed as a single isomer. A resonance at relatively high frequency (δ 9.73, 9.82, and 9.97, respectively) is assigned to a proton at position 6 on the pyridyl ring, the chemical shift suggesting relatively close proximity to the iodide ligand, by analogy with related systems.[10,11,17] This indicates that the unsymmetrical complexes **1d**−**f** adopt a stereochemistry with CO trans to the pyridyl nitrogen, as shown in Figure 1. This was confirmed by an X-ray crystal structure of **1f** (vide infra).

^{1}H NMR spectroscopy also revealed some of the behavior of the diimine ligand aryl substituents. For **1e**, the single *o*-^{i}Pr group exhibits two distinct doublets due to magnetically inequivalent methyls. This inequivalence arises from restricted rotation about the N−C(aryl) bond, due to steric hindrance by the cis-coordinated CO ligand and the ligand backbone methyl substituent. Likewise, **1f** shows two doublets for its *o*-^{i}Pr groups. In this case each doublet arises from a pair of methyls on *different* ^{i}Pr groups related by mirror symmetry. For similar reasons, **1c** shows four doublets for its *o*-^{i}Pr groups. For **1a** the ligand backbone methyl substituents give rise to four singlets rather than the two observed for **1b**,**c**. This can be explained by the presence of approximately equal amounts of the two conformers shown in Figure 2, which do not interconvert rapidly on the NMR time scale due to the restricted rotation identified above. The eight doublets expected for the methyls of the ^{i}Pr groups of these conformers are observed (with some overlap).

The structure of complex **1f** was confirmed by X-ray crystallography. Figure 3 illustrates the square-planar geometry with CO trans to the pyridyl nitrogen, as suggested by spectroscopy. The bond distances and

(8) van Asselt, R.; Elsevier, C. J.; Smeets, W. J. J.; Spek, A. L.; Benedix, R. *Recl. Trav. Chim. Pays-Bas* **1994**, *113*, 88. van Asselt, R.; Elsevier, C. J.; Smeets, W. J. J.; Spek, A. L. *Inorg. Chem.* **1994**, *33*, 1521.

(9) Laine, T. V.; Klinga, M.; Leskela, M. *Eur. J. Inorg. Chem.* **1999**, 959. van Laren, M. W.; Duin, M. A.; Klerk, C.; Naglia, M.; Rogolino, D.; Pelagatti, P.; Bacchi, A.; Pelizzi, C.; Elsevier, C. J. *Organometallics* **2002**, *21*, 1546.

(10) Laine, T. V.; Piironen, U.; Lappalainen, K.; Klinga, M.; Aitola, E.; Leskela, M. *J. Organomet. Chem.* **2000**, *606*, 112.

(11) Meneghetti, S. P.; Lutz, P. J.; Kress, J. *Organometallics* **1999**, *18*, 2734.

(12) Köppl, A.; Alt, H. G. *J. Mol. Catal. A* **2000**, *154*, 45. Miller, K. J.; Kitagawa, T. T.; Abu-Omar, M. M. *Organometallics* **2001**, *20*, 4403.

(13) Keijsper, J.; Van der Poel, H.; Polm, L. H.; Van Koten, G.; Vrieze, K.; Seignette, P. F. A. B.; Varenhorst, R.; Stam, C. *Polyhedron* **1983**, *2*, 1111.

(14) Our attempts to complex a symmetrical diimine containing no ortho alkyl substituents (i.e. PhN═C(Me)C(Me)═NPh) to Rh in this manner were unsuccessful. The IR spectrum of the reaction solution indicated the presence of $[Rh(CO)_2I_2]^-$, suggesting formation of the bis-chelate complex $[Rh(diimine)_2]^+$ as the counterion.

(15) [Rh(CO)(α-diimine)Cl] complexes have been reported, but their reactivity toward MeI has not been explored: van der Poel, H.; Van Koten, G.; Vrieze, K. *Inorg. Chim. Acta* **1981**, *51*, 241.

(16) Mestroni, G.; Camus, A.; Zassinovich, G. *J. Organomet. Chem.* **1974**, *65*, 119.

(17) The Cl analogue of **2f** (prepared in a similar way from $[Rh(CO)_2Cl]_2$) displayed a resonance at δ 9.32 for H^6 on the pyridyl ring, compared to δ 9.97 in **2f**. This relatively large shift demonstrates the sensitivity of the H^6 resonance to the nature of the ligand cis to the pyridyl moiety: Rülke, R. E.; Delis, J. G. P.; Groot, A. M.; Elsevier, C. J.; van Leeuwen, P. W. N. M.; Vrieze, K.; Goubitz, K.; Schenk, H. *J. Organomet. Chem.* **1996**, *508*, 109.

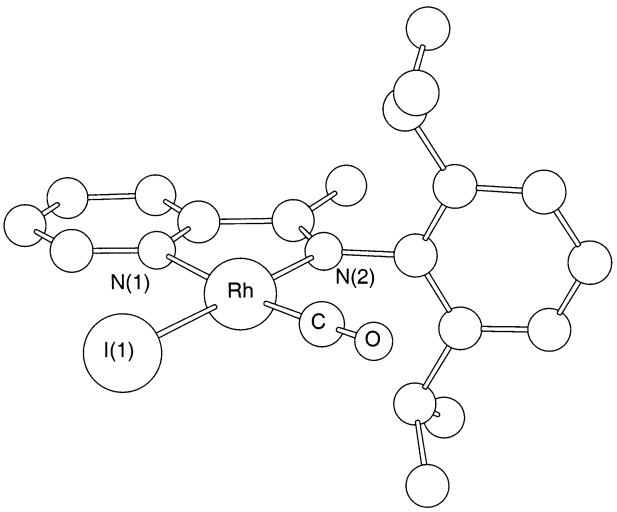

Figure 3. X-ray crystal structure of complex **1f** (H atoms and CH_2Cl_2 solvent molecule omitted).

Table 1. Selected Bond Lengths (Å) and Angles (deg) for Complexes 1f, 2a, 3c, and 4f

	1f	2a	3c	4f
Rh−N(1)	2.109(3)	2.07(2)	2.064(5)	2.068(8)
Rh−N(2)	2.023(3)	2.084(19)		2.121(8)
Rh−I(1)	2.6211(14)	2.643(2)	2.6285(7)	2.6705(13)
Rh−I(2)		2.7758(12)		2.6507(12)
Rh−I(3)				2.6956(13)
Rh−CO	1.818(4)	1.904(3)		1.897(13)
Rh−C_{Me}		2.115(13)		
Rh−C_{acetyl}			1.975(11)	
C−O	1.136(4)	1.103(3)	1.181(13)	1.074(12)
C_{acetyl}−C			1.541(17)	
N−Rh−N	77.79(10)	77.3(4)	77.7(3)	78.7(3)
L_{ax}−Rh−CO[a]		92.0(10)		96.1(3)
L_{ax}−Rh−N(1)[a]		89.9(8)	89.9(3)	84.8(2)
L_{ax}−Rh−N(2)[a]		87.6(9)		92.1(2)
L_{ax}−Rh−I_{cis} [a]		88.4(8)	98.2(3)	87.40(4)
L_{ax}−Rh−I_{trans} [a]		174.8(4)		170.42(4)
I(1)−Rh−I(2)		88.27(8)	89.94(3)	86.50(4)
O−C−Rh	178.2(3)	169.3(17)	121.3(9)	177.7(10)
C−C−Rh			117.2(9)	
I(1)−Rh−CO	88.84(12)	86.2(9)		83.2(3)

[a] L_{ax} is taken as C_{Me} for **2a**, C_{acetyl} for **3c**, and I(3) for **4f** on the basis of the atom labeling in Figures 4−6.

angles (Table 1) are within the expected range. As in related systems, the plane of the N-aryl group lies approximately perpendicular to the metal coordination plane.[3,8,18] This conformation places the two *o*-^{i}Pr groups in positions which hinder approach to the vacant axial coordination sites and is expected to influence reactivity in associative processes such as the oxidative addition reactions described below.

Oxidative Addition Reactions. When the reactions of **1a**−**g** with MeI were monitored by FTIR spectroscopy, it was apparent that the outcome depended on the steric properties of the ligand. For complexes containing ligands with relatively low steric bulk (**1a**,**d**,**e**,**g**), decay of the reactant ν(CO) band was accompanied by growth of an absorption at higher frequency (2070−2080 cm^{-1}) consistent with formation of the corresponding Rh(III) methyl product, [Rh(CO)(diimine)I_2Me] (**2a**,**d**,**e**,**g**). Oxidative addition of MeI to **1g** to give **2g** has been reported

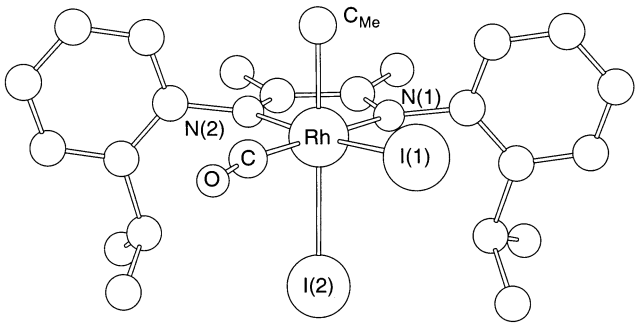

Figure 4. X-ray crystal structure of complex **2a** (H atoms and $CHCl_3$ solvent molecule omitted).

Scheme 2. Reactivity of Complexes 1a−g with MeI

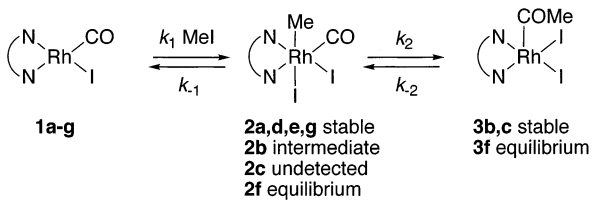

previously.[16] In contrast, for complexes **1b**,**c**, containing bulkier ligands, a band appeared near 1720 cm^{-1}, attributable to the acetyl products [Rh(diimine)I_2(COMe)] (**3b**,**c**). During the reaction of **1b**, a weak band at 2074 cm^{-1} was assigned to the methyl intermediate **2b**, but no corresponding intermediate was detected during the reaction of **1c**. In the reaction of **1f** with MeI, a band at 2073 cm^{-1} assigned to **2f** was observed to grow initially and then decay to attain an equilibrium with both the reactants and an acetyl product **3f**, which gave an IR absorption at 1716 cm^{-1}. The observed reactivity for **1a**−**g** is summarized in Scheme 2.

The methyl complexes **2a**,**e** and acetyl complexes **3b**,**c** were isolated and fully characterized, including X-ray crystal structures for **2a** and **3c**. Spectroscopic characterization of **2d**,**f** and **3f** was obtained from in situ NMR experiments. The ^{1}H NMR spectrum of **2a** in CD_2Cl_2 exhibited four doublets in the region δ 1.6−1.8 (each with $^2J_{RhH}$ = 2 Hz) in the ratio ca. 4:2:2:1. These are assigned to the methyl ligands of four different conformers or isomers of **2a**. Assuming a coordination geometry with methyl trans to iodide (as found in the solid state; vide infra), there are four possible conformers of **2a** with different orientations of the two *o*-^{i}Pr groups. Alternatively, geometrical isomers might give rise to the multiple methyl resonances. The major conformer/isomer gave a pair of singlets at δ 2.26 and 2.24 for inequivalent methyl substituents on the diimine ligand backbone, with a number of other singlets due to the minor species also occurring in this region. Up to 16 doublets could arise from the ^{i}Pr group methyls of 4 species, and 9 of these were resolved in the region δ 1.08−1.42. It was found that the ν(CO) band of **2a** shifted from 2077 to 2070 cm^{-1} over several hours in CH_2Cl_2, probably due to a slow isomerization process.

A crystal of **2a** suitable for an X-ray diffraction study was obtained by recrystallization from chloroform. The solid-state structure, shown in Figure 4, reveals a single isomer with a pseudo-octahedral geometry. Selected geometric data are given in Table 1. Again the N-aryl

(18) Hill, G. S.; Yap, G. P. A.; Puddephatt, R. J. *Organometallics* **1999**, *18*, 1408. Kokkes, M. W.; Stufkens, D. J.; Oskam, A. *J. Chem. Soc., Dalton Trans.* **1983**, 439.

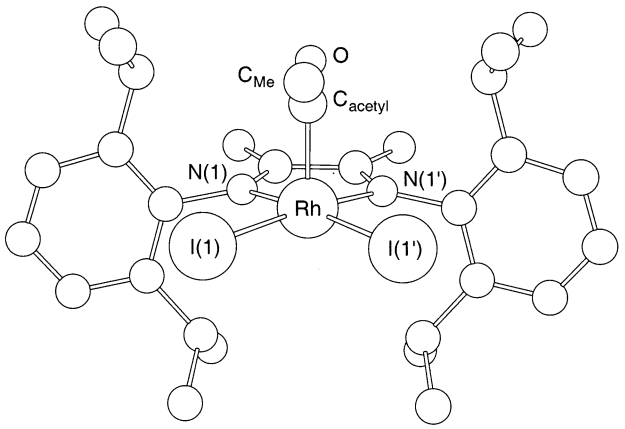

Figure 5. X-ray crystal structure of complex **3c** (H atoms and CH_2Cl_2 solvent molecule omitted).

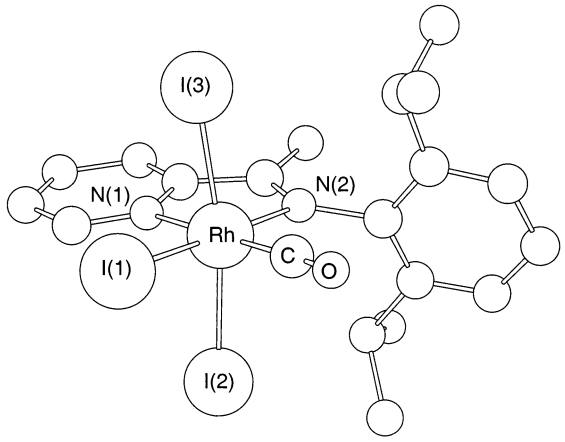

Figure 6. X-ray crystal structure of complex **4f** (H atoms omitted).

groups are oriented approximately perpendicular to the plane of the chelate ring, in this case a slight canting (ca. 4° from perpendicular) being apparent. A conformation is adopted in which both *o*-^{i}Pr groups are directed toward the axial iodide ligand (the equatorial plane taken as that containing Rh and both N atoms). The resulting nonbonded interactions cause the N-aryl groups to bend away from the axial iodide, as reflected in the significant difference in $C_{ortho}-C_{ortho}$ distances (7.27 and 6.37 Å) between the two rings. The methyl ligand occupies the other axial coordination site, which is sterically uncongested. On the grounds of ligand cone angles (90° for Me, 107° for I[19]) a conformation with the two *o*-^{i}Pr groups directed toward the methyl ligand would have been expected. The observed structure might be favored by weak intramolecular H-bonding interactions between the ^{i}Pr methine groups and the axial iodide ligand, although the solution NMR spectrum of **2a** suggests that other conformers are accessible.

The ^{1}H NMR spectra of **2d**−**f** all displayed high-frequency resonances (near δ 10.2) consistent with a hydrogen in position 6 on the pyridyl ring adjacent to a cis iodide ligand, as in the precursors **1d**−**f**. Although the rest of the coordination geometry is not proven by the data for these complexes, it is likely that CO is trans to the pyridyl N, with MeI being added in a trans fashion. For **2e**, there was evidence for two conformers or isomers in solution, each of which displayed a pair of doublets for the inequivalent methyls of its ^{i}Pr group. In the reaction of **1f** with MeI in CD_2Cl_2, ^{1}H NMR spectroscopy indicated the presence of three isomers of the methyl intermediate **2f** in equilibrium with the acetyl product **3f**, which displayed a signal at δ 3.30 for the acetyl ligand.

The stable acetyl products **3b**,**c**, which resulted from addition of MeI to **1b**,**c**, both displayed ^{1}H resonances at δ 3.24 for their acetyl ligands. In each case the ^{1}H NMR signals due to the diimine are consistent with C_s symmetry, with the Rh atom and the acetyl ligand lying on the mirror plane. The observation of two signals for pairs of inequivalent *o*-Me groups in **3b** and four signals for methyls of the *o*-^{i}Pr groups of **3c** again indicate restricted rotation about the N−C(aryl) bonds. The X-ray crystal structure of **3c** is illustrated in Figure 5, and selected geometric data are given in Table 1. The complex displays a distorted-square-pyramidal geometry with an apical acetyl ligand, as commonly found in related complexes.[6,20] The Rh acetyl fragment lies on a mirror plane with its methyl group directed away from the sterically congested region created by two *o*-^{i}Pr groups. The diimine ligand flexes to accommodate the acetyl ligand and displays an even larger difference in $C_{ortho}-C_{ortho}$ distances (7.33 and 6.15 Å) between the two rings than in **2a**. Comparison of the structures of **2a** and **3c** clearly demonstrates that formation of **3c** from the undetected intermediate **2c** is driven by relief of steric congestion created by the four *o*-^{i}Pr substituents on the diimine.

Complex **1f** was found to undergo a facile reaction with I_2 to give the triiodide product [Rh(CO)(2,6-^{i}Pr$_2$C$_6$H$_3$N=C(Me)-2-py)I$_3$] (**4f**). The X-ray crystal structure of **4f**, shown in Figure 6, reveals a distorted-octahedral geometry with the CO ligand again trans to the pyridyl nitrogen. The plane of the N-aryl group is canted ca. 16° from the position perpendicular to the chelate ring. This minimizes the steric interaction between one ^{i}Pr group and I(2), but nonbonded interactions of I(3) with the other ^{i}Pr group cause a significant distortion from ideal octahedral geometry. This is exemplified by the I(3)−Rh−CO and I(2)−Rh−I(3) bond angles of 96.1(3) and 170.42(4)°, respectively. Similar steric interactions can explain the relative instability of the methyl complex **2f**, which contains the same bidentate ligand as **4f**.

Kinetic Measurements. Kinetic experiments were carried out using FTIR spectroscopy to monitor the reactions of **1a**−**g** with MeI in CH_2Cl_2. Pseudo-first-order rate constants, measured over a range of MeI concentrations and temperatures, are given in the Supporting Information. All the oxidative addition reactions were found to be first order in both [complex] and [MeI]. Second-order rate constants (k_1) and activation parameters are given in Table 2. The large negative $\Delta S^{\ddagger}$ values are consistent with highly ordered S_N2 transition states for attack by Rh(I) on MeI. The oxidative addition rate is very sensitive to the steric bulk of the diimine

(19) Tolman, C. A. *Chem. Rev.* **1977**, *77*, 313.

(20) Moloy, K. G.; Petersen, J. L. *Organometallics* **1995**, *14*, 2931. Adams, H.; Bailey, N. A.; Mann, B. E.; Manuel, C. P. *Inorg. Chim. Acta* **1992**, *198*−*200*, 111. Søtofte, I.; Hjortkjaer, J. *Acta Chem. Scand.* **1994**, *48*, 872. Smith, J. M.; Lachicotte, R. J.; Holland, P. L. *Organometallics* **2002**, *21*, ASAP.

Table 2. Kinetic Data for Oxidative Addition of MeI to Complexes 1a−g

complex	ν(CO)	$10^3 k_1$/M^{-1} s^{-1}	$\Delta H^{\ddagger}$/kJ mol^{-1}	$\Delta S^{\ddagger}$/J mol^{-1} K^{-1}
1a	1994	12.0	35 ± 1	−162 ± 4
1b	1993	1.02	42 ± 1	−160 ± 2
1c	1993	0.145	41 ± 1	−182 ± 2
1d	1989	140	25 ± 2	−176 ± 6
1e	1988	88.5	27 ± 1	−175 ± 4
1f	1987	8.34	25 ± 3	−201 ± 10
1g	1977	206	18 ± 1	−199 ± 4

ligand, with values of k_1 spanning more than 3 orders of magnitude, as illustrated by a plot of log k_1 vs the number of ortho substituents (Figure 7). Replacing four *o*-^{i}Pr groups (**1c**) by four Me groups (**1b**) leads to a 7-fold rate enhancement, very similar to the 5-fold acceleration of C_2H_4 exchange that occurs for an equivalent change in ligand structure in $[Pd(C_2H_4)(diimine)Me]^+$.[3] This reflects the operation of an associative mechanism for each process with a MeI or C_2H_4 molecule experiencing similar steric interactions on approaching an axial coordination site. Replacement of an *o*-^{i}Pr group on each aryl by H results in a ca. 80-fold acceleration in **1a** relative to **1c**. Complexes **1a**,**f**, each of which has two *o*-^{i}Pr groups (either on the same or different aryl groups), display very similar oxidative addition rates. Removal of one *o*-^{i}Pr group from **1f** to give **1e** gives a further order of magnitude increase in reactivity, whereas removal of the single *o*-^{i}Pr group of **1e** to give **1d** results in a more modest acceleration, by a factor of ca. 1.6. The highest reactivity of all is shown by the sterically unhindered bipy complex **1g**, for which k_1 is the largest yet reported for a Rh(I) carbonyl complex,[21] exceeding that for the carbonylation catalyst $[Rh(CO)_2I_2]^-$ [22] by a factor of ca. 7000. The dependence of oxidative addition rate on ligand steric bulk shown in Figure 7 resembles the steric profile, proposed by Eriks et al., for reactions in which the ground state is less congested and more flexible than the transition state.[23] The complexes **1a**,**c**,**e**,**f** show a good linear correlation of log k_1 with ligand size, whereas the relatively small rate enhancement caused by removing the final *o*-^{i}Pr group from **1e** to give **1d** represents the onset of a steric threshold.

Our kinetic data show that N-donor ligands impart very high nucleophilicity on a Rh(I) center (as found in systems which will activate C−Cl bonds[24]) but this is moderated by the presence of bulky ligand substituents.[25] However, even the most hindered complex, **1c**, reacts with MeI ca. 5 times faster than $[Rh(CO)_2I_2]^-$. Ligand *o*-^{i}Pr substituents have previously been found to hinder oxidative addition of organic halides to [Pd(Ar-BIAN)Me$_2$] and lower the stability of Pd(IV) complexes [Pd(Ar-BIAN)Me$_3$I] toward reductive elimination.[26]

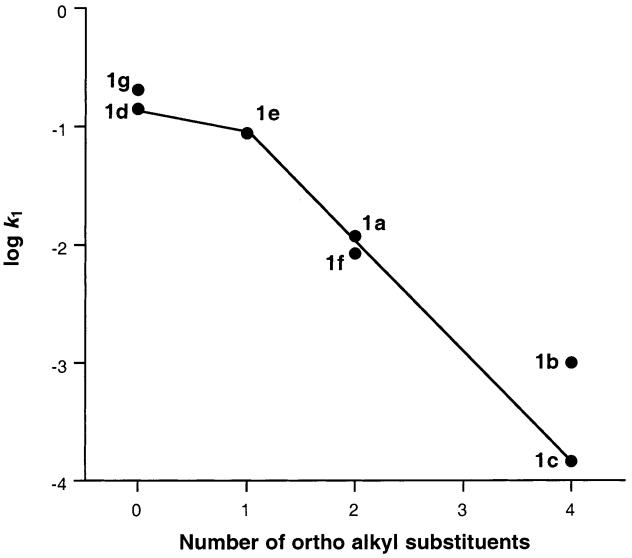

Figure 7. Effect of ligand steric bulk on rate constant for the oxidative addition of MeI to complexes **1a**−**g**.

Both the kinetics and thermodynamics of migratory CO insertion are influenced by ligand steric effects. In the extreme cases, values of k_2 were not measurable, since the octahedral methyl complex was either stable (**2a**,**d**,**e**,**g**) or not detectable (**2c**).[27] However, for two systems possessing intermediate steric bulk, kinetic data were obtained. During the reaction of **1b** with MeI, the intermediate **2b** was detected at relatively low concentration. Using the method applied previously,[6,22] we have estimated k_2 for **2b** as]5.7 (±0.2)] × 10^{-2} s^{-1} (25 °C) with activation parameters $\Delta H^{\ddagger}$ = 53 (±4) kJ mol^{-1} and $\Delta S^{\ddagger}$ = −93 (±7) J mol^{-1} K^{-1}.[28] The rate constant is very similar to that for $[Rh(CO)_2I_3Me]^-$ (5.4 × 10^{-2} s^{-1}).[22]

For the reaction of MeI with **1f**, which resulted in equilibria, the time dependences of species **1f**, **2f**, and **3f** were fitted to a two-step reversible kinetic model (Scheme 2), giving values for each of the forward and reverse rate constants (listed in the Supporting Information). The value of k_2 for **2f** (5.82 × 10^{-4} s^{-1}, 25 °C) is ca. 100 times smaller than that for **2b**. Activation parameters for migratory insertion in **2f** are $\Delta H^{\ddagger}$ = 81 (±3) kJ mol^{-1} and $\Delta S^{\ddagger}$ = −37 (±11) J mol^{-1} K^{-1}. Thermodynamic data were also estimated. Oxidative addition of MeI to **1f** is exothermic (ΔH = −41 (±8) kJ mol^{-1}), but the negative reaction entropy (ΔS = −115

(21) Very high nucleophilicity toward MeI (k = 2000 M^{-1} s^{-1}) has been reported for a square-planar Rh(I) complex containing a macrocycle formed from two linked diimines: Collman, J. P.; Brauman, J. I.; Madonik, A. M. *Organometallics* **1986**, *5*, 310.

(22) Haynes, A.; Mann, B. E.; Morris, G. E.; Maitlis, P. M. *J. Am. Chem. Soc.* **1993**, *115*, 4093.

(23) Eriks, K.; Giering, W. P.; Liu, H.-Y. *Inorg. Chem.* **1989**, *28*, 1759.

(24) Haarman, H. F.; Ernsting, A. L.; Kranenburg, M.; Kooijman, H.; Veldman, N.; Spek, A. L.; Elsevier, C. J.; van Leeuwen, P. W. N. M.; Vrieze, K. *Organometallics* **1997**, *16*, 887. Haarman, H. F.; Kaagman, J.-W.; Smeets, W. J. J.; Spek, A. L.; Vrieze, K. *Inorg. Chim. Acta* **1998**, *270*, 34. Bradd, K. J.; Heaton, B. T.; Jacob, C.; Sampanthar, J. T.; Steiner, A. *J. Chem. Soc., Dalton Trans.* **1999**, 1109. Nishiyama, H.; Horihata, M.; Hirai, T.; Wakamatsu, S.; Itoh, K. *Organometallics* **1991**, *10*.

(25) It was noted recently that Rh(I) complexes of some terdentate nitrogen ligands add MeI but are stable in chlorinated solvents if the ligand is sufficiently bulky. Dias, E. L.; Brookhart, M.; White, P. S. *Organometallics* **2000**, *19*, 4995; *Chem. Commun.* **2001**, 423.

(26) van Asselt, R.; Rijnberg, E.; Elsevier, C. J. *Organometallics* **1994**, *13*, 706.

(27) Since no methyl intermediate was observed during the reaction of **1c** with MeI, the migratory insertion rate constants for **2c** could not be determined. However, if we assume that to avoid detection, the steady-state concentration of **2c** is less than 1% of [**1c**], a lower limit for k_2 can be estimated as 10^{-1} s^{-1} for **2c** (25 °C). This is double that measured for **2b** and an order of magnitude larger than that for $[Rh(CO)_2I_3Me]^-$.[22]

(28) The negative $\Delta S^{\ddagger}$ value (−93 (±7) J mol^{-1} K^{-1}) measured for migratory insertion in **2b** is larger than might be expected for an intramolecular rearrangement. We note that values of ca. −60 J mol^{-1} K^{-1} have been reported previously for related species.[6,22] Participation by a solvent molecule which coordinates weakly to the vacant site formed during migratory insertion may make some contribution to these values. However, we cannot rule out the possibility that the indirect method used to measure k_2 for **2b** and the relatively narrow temperature range for the Eyring plot may lead to some inaccuracy in the extrapolation required to extract $\Delta S^{\ddagger}$.

(±26) J mol^{-1} K^{-1}) leads to the observed equilibrium. Migratory insertion, **2f** → **3f**, is slightly endothermic (ΔH = 10 (±8) kJ mol^{-1}, ΔS = +45 (±27) J mol^{-1} K^{-1}). The different reactivities of **2a**,**f** show that the effect of two *o*-^{i}Pr substituents depends on how they are distributed. In **2a** the two ^{i}Pr groups can adopt a conformation in which both are directed toward the same axial site (Figure 4) and a stable methyl complex results. In **2f**, however, both axial ligands experience adverse steric effects (as observed in the X-ray crystal structure of **4f**) and destabilization of the octahedral species results in the observed equilibria.

Ligand steric effects on migratory CO insertion in this system are much larger than for alkene insertion in [Pd(diimine)(R)(C_2H_4)]$^+$, where $\Delta G^{\ddagger}$ varied by less than 7 kJ mol^{-1} for different diimines.[3] This is explained by the different coordination geometries, since olefin insertion occurs in the equatorial plane for the Pd(II) systems, with *o*-alkyl substituents exerting less influence. Octahedral complexes such as **2b**,**c** experience a much larger relief of steric strain on isomerizing to the square-pyramidal acetyl products.

Conclusions

We have identified a system in which the steric effects of diimine ligands can be tested and quantified. The N,N donor set imparts high intrinsic nucleophilicity on the Rh(I) center, with bipy giving the fastest rate of MeI addition to a Rh(I) carbonyl complex yet reported. Replacement of bipy with diimine ligands of increasing steric bulk moderates the oxidative addition rate over 3 orders of magnitude in a predictable manner. Ligand steric effects also have a dramatic influence on the kinetics and thermodynamics of migratory CO insertion, due to nonbonded interactions of *o*-alkyl substituents with axially coordinated ligands. Depending on the ligand, the octahedral methyl complex either is stable and isolable or is undetected due to rapid isomerization to a square-pyramidal acetyl complex.

Experimental Section

Materials. All solvents used for synthesis or kinetic experiments were distilled and degassed prior to use following literature procedures.[29] Synthetic procedures were carried out utilizing standard Schlenk techniques. Nitrogen and carbon monoxide were dried through a short (20 × 3 cm diameter) column of molecular sieves (4 Å) which was regularly regenerated. Carbon monoxide was also passed through a short column of activated charcoal to remove any iron pentacarbonyl impurity.[30] The ligands ArN=C(Me)C(Me)=NAr and ArN=C(Me)-2-py (Ar = Ph, 2-^{i}PrC_6H_4, 2,6-$^{i}Pr_2C_6H_3$) were prepared by condensation of the appropriate aniline derivative with 2,3-butanedione or 2-acetylpyridine (Aldrich) using established procedures.[31] Comparison with published spectroscopic data established the identity and purity of the pyridyl imines.[10,12] The ligand 2,2-bipyridyl was purchased from Aldrich and used without further purification. The complexes $[Rh(CO)_2Cl]_2$[32] and $[Rh(CO)_2I]_2$ [33] were synthesized according to literature procedures. Methyl iodide (Aldrich) was distilled over calcium hydride and stored in foil-wrapped Schlenk tubes under nitrogen and over mercury to prevent formation of I_2.

Instrumentation. FTIR spectra were measured using a Mattson Genesis Series spectrometer, controlled by WINFIRST software running on a Viglen 486 PC. ^{1}H NMR spectra were obtained using a Bruker AC250 spectrometer fitted with a Bruker B-ACS60 automatic sample changer operating in pulse Fourier transform mode, using the solvent as reference. Elemental analyses were performed using a Perkin-Elmer Model 2400 elemental analyzer.

Synthesis of Rh(I) Complexes. (a) [Rh(CO)(ArN=C(Me)C(Me)=NAr)I] (1a; Ar = 2-^{i}PrC$_6$H$_4$). $[Rh(CO)_2I]_2$ (0.100 g, 0.18 mmol), was dissolved in 5 cm^3 of THF. A solution of ArN=C(Me)C(Me)=NAr (Ar = 2-^{i}PrC_6H_4; 0.112 g, 0.39 mmol) in the same amount of THF was then added dropwise under N_2. The dark blue solution obtained was stirred under N_2 for 2 min. The solvent was then removed in vacuo, and the resulting dark blue solid was dried under vacuum for 24 h; yield 0.167 g (84%). Anal. Calcd for $C_{23}H_{28}IN_2ORh$: C, 47.8; H, 4.8; N, 4.9; I, 22.0. Found: C, 47.3; H, 5.0; N, 4.6; I, 22.0. IR (CH_2Cl_2; ν(CO)/cm^{-1}): 1994. ^{1}H NMR (CD_2Cl_2; δ): 7.47−7.25, 7.01, 6.88 (each m, total 8H, arom), 3.50−3.30 (m, 2H, MeC*H*Me), 1.83, 1.82 (each s, total 3H, N=C(*Me*)C(Me′)=N, 2 conformers, ca. 1:1 ratio), 1.23, 1.22 (each s, total 3H, N=C(Me)C(*Me*′)=N, 2 conformers), 1.43 (d) 1.39 (d), 1.34 (2 overlapping d), 1.18 (d), 1.14 (d), 1.09 (d), 1.06 (d) (each 7 Hz, total 12H, *Me*CHMe, 8 doublets for 2 conformers).

(b) [Rh(CO)(ArN=C(Me)C(Me)=NAr)I] (1b; Ar = 2,4,6-Me$_3$C$_6$H$_2$). $[Rh(CO)_2I]_2$ (0.100 g, 0.17 mmol) was dissolved in 5 cm^3 of CH_2Cl_2 and added to a solution of ArN=C(Me)C(Me)=NAr)] (Ar = 2,4,6-$Me_3C_6H_2$; 0.112 g, 0.34 mmol) in the same amount of CH_2Cl_2 under N_2. The dark blue solution obtained was stirred under N_2 for 2 h. The solvent was then removed in vacuo, and the resulting dark blue solid was dried under vacuum for 24 h; yield 0.165 g (82%). Anal. Calcd for $C_{23}H_{28}IN_2ORh$: C, 47.8; H, 4.8; N, 4.9, I, 22.0. Found: C, 47.3; H, 4.6; N, 4.6; I, 22.5. IR (CH_2Cl_2; ν(CO)/cm^{-1}): 1993. ^{1}H NMR (CD_2Cl_2; δ): 6.92, 6.87 (each s, total 4H, *m*-H), 2.26 (s, 6H, *p*-Me), 2.21, 2.07 (each s, total 6H, *o*-Me), 1.64 (s, 3H, N=C(*Me*)C(Me′)=N), 1.04 (s, 3H, N=C(Me)C(*Me*′)=N).

(c) [Rh(CO)(ArN=C(Me)C(Me)=NAr)I] (1c; Ar = 2,6-^{i}Pr$_2$C$_6$H$_3$). $[Rh(CO)_2I]_2$ (0.100 g, 0.17 mmol) was dissolved in 5 cm^3 of CH_2Cl_2 and added to a solution of ArN=C(Me)C(Me)=NAr (Ar = 2,6-$^{i}Pr_2C_6H_3$; 0.151 g, 0.34 mmol) in the same amount of CH_2Cl_2. The dark blue solution obtained was stirred under nitrogen for 2.5 h. The solvent was then removed in vacuo, and the resulting dark blue solid was dried under vacuum for 24 h; yield 0.194 g (80%). Anal. Calcd for $C_{29}H_{40}IN_2ORh$: C, 52.6; H, 6.0; N, 4.2; I, 19.1. Found: C, 53.1; H, 6.2; N, 4.3; I, 18.6. IR (CH_2Cl_2; ν(CO)/cm^{-1}): 1993. ^{1}H NMR (CD_2Cl_2; δ): 7.31−7.13 (m, 6H, arom.), 3.16, 3.02 (overlapping septets, 7 Hz, each 1H, MeC*H*Me), 1.73 (s, 3H, N=C(*Me*)C(Me′)=N), 1.10 (s, 3H, N=C(Me)C(*Me*′)=N), 1.35, 1.12, 1.27, 1.07 (each d, 7 Hz, 6H, *Me*CHMe).

(d) [Rh(CO)(PhN=C(Me)-2-py)I] (1d). $[Rh(CO)_2I]_2$ (0.150 g, 0.27 mmol) was dissolved in 10 cm^3 of THF. A solution of PhN=C(Me)-2-py (0.114 g, 0.58 mmol) in 10 cm^3 of THF was added dropwise by cannula under N_2. The solution became dark purple, and the mixture was stirred under N_2 for 2 h. The solvent was removed in vacuo and the resulting dark purple solid dissolved in CH_2Cl_2 (20 cm^3) and stirred for a further 2 h to complete the reaction. The solvent was then removed in vacuo, and the product was recrystallized by dissolution in the minimum amount of THF (4 cm^3) and precipitation by addition of pentane (50 cm^3). The solvent was

(29) Perrin, D. D.; Armerego, W. L. F.; Perrin, D. R. *Purification of Laboratory Chemicals*, 3rd ed.; Pergamon Press: Oxford, U.K., 1988.
(30) Haynes, A.; Ellis, P. R.; Byers, P. K.; Maitlis, P. M. *Chem. Br.* **1992**, *28*, 517.
(31) Weidenbruch, M.; Piel, H.; Lesch, A.; Peters, K.; Vonschnering, H. *J. Organomet. Chem.* **1993**, *454*, 35. Ferguson, L. N.; Goodwin, T. C. *J. Am. Chem. Soc.* **1949**, *71*, 633. Svoboda, M.; tom Dieck, H. *J. Organomet. Chem.* **1980**, *191*, 321. tom Dieck, H.; Svoboda, M.; Greiser, T. *Z. Naturforsch., B* **1981**, *36b*, 823.
(32) McCleverty, J.; Wilkinson, G. *Inorg. Synth.* **1966**, *8*, 214.
(33) Fulford, A.; Hickey, C. E.; Maitlis, P. M. *J. Organomet. Chem.* **1990**, *398*, 311.

removed by cannula and the resulting solid dried under vacuum for 24 h; yield 0.183 g (75%). Anal. Calcd for ($C_{14}H_{12}IN_2ORh$): C, 37.03; H, 2.66; N, 6.17. Found: C, 37.42; H, 2.90; N, 6.28. IR (CH_2Cl_2; ν(CO)/cm^{-1}): 1989. ^{1}H NMR (CD_2Cl_2; δ): 9.73 (bd, 1H), 7.97 (m, 1H), 7.78 (m, 1H), 7.65 (m, 1H), 7.41 (m, 2H), 7.25 (m, 1H), 7.12 (m, 2H) (arom), 1.78 (s, 3H, C(*Me*)═N).

(e) [Rh(CO)(ArN═C(Me)-2-py)I] (1e; Ar = 2-^{i}PrC$_6$H$_4$). [Rh(CO)$_2$I]$_2$ (0.100 g, 0.18 mmol) was dissolved in 15 cm^3 of THF. A solution of ArN═C(Me)-2-py (Ar = 2-^{i}PrC$_6$H$_4$; 0.093 g, 0.39 mmol) in 10 cm^3 of THF was added dropwise by cannula under N_2. The solution became dark purple, and the mixture was stirred for 30 min. The solvent was then removed in vacuo, and the resulting dark purple solid was recrystallized by dissolution in the minimum amount of THF (3 cm^3) and precipitation by addition of pentane (50 cm^3). The solvent was then removed by cannula and the resulting solid dried under vacuum for 24 h; yield 0.145 g (84%). Anal. Calcd for ($C_{17}H_{18}IN_2ORh$): C, 41.15; H, 3.66; N, 5.65. Found: C, 41.00; H, 3.66; N, 5.38. IR (CH_2Cl_2; ν(CO)/cm^{-1}): 1988. ^{1}H NMR (CD_2Cl_2; δ): 9.82 (m, 1H), 8.04 (m, 1H), 7.83 (m, 1H), 7.74 (m, 1H), 7.42 (bm, 1H), 7.30 (m, 2H), 6.99 (m, 1H) (arom), 3.47 (m, 1H, Me$_2$*CH*), 1.79 (s, 3H, C(*Me*)═N), 1.39, 1.12 (each d, 7 Hz, 3H, *Me*$_2$CH).

(f) [Rh(CO)(ArN═C(Me)-2-py)I] (1f; Ar = 2,6-^{i}Pr$_2$C$_6$H$_3$). [Rh(CO)$_2$I]$_2$ (0.100 g, 0.18 mmol) was dissolved in 10 cm^3 of pentane. A solution of ArN═C(Me)-2-py (Ar = 2,6-^{i}Pr$_2$C$_6$H$_3$; 0.109 g, 0.39 mmol) in the same amount of pentane was added dropwise by cannula under N_2. A dark purple precipitate was observed, and the mixture was stirred for 30 min. The solvent was then removed in vacuo, and the resulting dark purple solid was dried under vacuum for 24 h; yield 0.155 g (80%). Anal. Calcd for $C_{20}H_{24}IN_2ORh$: C, 44.6; H, 4.5; N, 5.2. Found: C, 45.0; H, 4.6; N, 5.2. IR (CH_2Cl_2; ν(CO)/cm^{-1}): 1987. ^{1}H NMR ($CDCl_3$; δ): 9.97 (m, 1H), 8.03 (m, 1H), 7.82−7.74 (m, 2H), 7.22−7.35 (bm, 3H) (arom), 3.32 (m, 2H, Me$_2$*CH*), 1.73 (s, 3H, C(*Me*)═N), 1.38, 1.12 (each d, 7 Hz, 6H, *Me*$_2$CH). A single crystal of **1f** suitable for X-ray diffraction (vide infra) was obtained by recrystallization from dichloromethane.

(g) [Rh(CO)(2,2′-bipy)I] (1g). [Rh(CO)$_2$I]$_2$ (0.100 g, 0.18 mmol) was dissolved in 50 cm^3 of THF. A solution of 2,2′-bipyridyl (0.061 g, 0.39 mmol) in 50 cm^3 of THF was added dropwise by cannula under N_2. The solution became deep red, and the mixture was stirred for 10 min. The solvent was then removed in vacuo, and the resulting deep red solid was dried under vacuum for 24 h; yield 0.104 g (70%). IR (CH_2Cl_2; ν(CO)/cm^{-1}): 1977. ^{1}H NMR ($CDCl_3$; δ): 9.83 (m, 1H), 8.84 (m, 1H), 7.95−8.16 (m, 4H), 7.54 (m, 1H), 7.39 (m, 1H).

Synthesis of Rh(III) Complexes. (a) [Rh(CO)(ArN═C(Me)-C(Me)═NAr)I$_2$Me] (2a; Ar = 2-^{i}PrC$_6$H$_4$). [Rh(CO)(ArN═C(Me)C(Me)═NAr)I] (**1a**; Ar = 2-^{i}PrC$_6$H$_4$; 0.100 g, 0.18 mmol) was dissolved in CH_2Cl_2 (5 cm^3) to which MeI (0.5 cm^3, excess) was added under N_2. The reaction mixture was stirred at room temperature for 1 h, during which time the color turned from dark blue to bright red. The solvent was removed in vacuo, and the product was dried under high vacuum; yield 0.090 g (72%). Anal. Calcd for $C_{24}H_{31}I_2N_2ORh$: C, 40.0; H, 4.3; N, 3.9; I, 35.3. Found: C, 39.9; H, 4.5; N, 3.7; I, 34.9. IR (CH_2Cl_2; ν(CO)/cm^{-1}): 2077. ^{1}H NMR (CD_2Cl_2; δ): 8.55, 8.24, 7.57−7.28, 7.04, 6.78 (each m, total 8H, arom), 3.82, 3.51, 2.61 (each m, total 2H, MeC*H*Me), 2.27, 2.26, 2.24, 2.23, 2.19, 2.12 (each s, total 6H, N═C(*Me*)C(*Me′*)═N, mixture of conformers/isomers), 1.75, 1.73, 1.65, 1.63 (each d, $^2J_{RhH}$ = 2 Hz, total 3H, *Me*Rh, 4 isomers/conformers, ratio ca. 4:2:2:1), 1.42, 1.38, 1.36, 1.33, 1.29, 1.24, 1.18, 1.14, 1.08 (each d, J = 6−7 Hz, total 12H, *Me*CH*Me*, mixture of conformers/isomers). A single crystal of **2a** suitable for X-ray diffraction (vide infra) was obtained by recrystallization from chloroform.

(b) [Rh(ArN═C(Me)C(Me)═NAr)I$_2$(COMe)] (3b; Ar = 2,4,6-Me$_3$C$_6$H$_2$). [Rh(CO)(ArN═C(Me)-C(Me)═NAr)I] (**1b**; Ar = 2,4,6-Me$_3$C$_6$H$_2$; 0.050 g, 0.09 mmol) was dissolved in CH_2Cl_2 (5 cm^3) to which MeI (0.5 cm^3, excess) was added under N_2. The reaction mixture was stirred at room temperature for 3 h, during which time the color turned from dark blue to red-purple. The solvent was removed in vacuo, and the product was washed with diethyl ether and vacuum-dried; yield 0.040 g (64%). Anal. Calcd for $C_{24}H_{31}I_2N_2ORh$: C, 39.7; H, 4.3; N, 3.6; I, 35.6. Found: C, 40.0; H, 4.3; N, 3.9; I, 35.3. IR (CH_2Cl_2; ν(CO)/cm^{-1}): 1721. ^{1}H NMR (CD_2Cl_2; δ): 6.92, 6.88 (each s, total 4H, *m*-H), 3.24 (s, 3H, CO*Me*), 2.26 (s, 6H, *p*-Me), 1.96, (s, 6H, N═C(*Me*)C(*Me*)═N), 1.92, 1.86 (each s, total 6H, *o*-Me).

(c) [Rh(ArN═C(Me)C(Me)═NAr)I$_2$(COMe)] (3c; Ar = 2,6-^{i}Pr$_2$C$_6$H$_3$). [Rh(CO)(ArN═C(Me)C(Me)═NAr)I] (**1c**; Ar = 2,6-^{i}Pr$_2$C$_6$H$_3$; 0.050 g, 0.09 mmol) was dissolved in CH_2Cl_2 (5 cm^3) to which MeI (0.5 cm^3, excess) was added under N_2. The reaction mixture was stirred at room temperature for 24 h, during which time the color turned from dark blue to deep red. The solvent was removed in vacuo, and the product was then recrystallized from CH_2Cl_2 and dried under high vacuum; yield 0.039 g (56%). Anal. Calcd for $C_{30}H_{43}I_2N_2ORh\cdot CH_2Cl_2$: C, 44.0; H, 5.3; N, 3.3; I, 30.0. Found: C, 43.8; H, 5.2; N, 3.2; I, 29.7. IR (CH_2Cl_2; ν(CO)/cm^{-1}): 1713. ^{1}H NMR (CD_2Cl_2; δ): 7.31−7.13 (m, 6H, arom), 3.24 (s, 3H, CO*Me*), 2.60, 2.40 (each sept, 7 Hz, 1H, MeC*H*Me), 2.08 (s, 6H, N═C(*Me*)C(*Me′*)═N), 1.25, 1.16, 1.12, 0.94 (each d, 7 Hz, 6H, *Me*CHMe). A single crystal of **3c** suitable for X-ray diffraction (vide infra) was obtained by recrystallization from dichloromethane.

(d) [Rh(CO)(PhN═C(Me)-2-py)I$_2$Me] (2d). In an in situ NMR experiment, [Rh(CO)(PhN═C(Me)-2-py)I] (**1d**; 16 mg) was dissolved in CD_2Cl_2 (0.7 cm^3) in an NMR tube, to which was added methyl iodide (10-fold excess/**1d**) at room temperature. The initial ^{1}H NMR spectrum revealed a doublet at δ 1.57 ($^2J_{Rh-H}$ = 2.1 Hz, 3H) for the methyl ligand of the oxidative addition product **2d**. A characteristic signal at δ 10.25 (m, 1H) is assigned to the hydrogen at position 6 on the pyridyl ring. A weak singlet was also observed at δ 3.26, corresponding to a small amount of the acetyl product **3d**. IR (CH_2Cl_2; ν(CO)/cm^{-1}): 2078 (**2d**).

(e) [Rh(CO)(ArN═C(Me)-2-py)I$_2$Me] (2e; Ar = 2-^{i}PrC$_6$H$_4$). [Rh(CO)(ArN═C(Me)-2-py)I] (**1e**; Ar = 2-^{i}PrC$_6$H$_4$; 0.040 g, 0.08 mmol) and MeI (75 μL, 1.2 mmol, excess) were dissolved in THF (10 cm^3), and the solution was stirred under N_2 for 30 min. The solvent was then removed in vacuo, and the resulting orange solid was recrystallized by dissolution in the minimum amount of THF (2.25 cm^3) and addition of pentane (30 cm^3). The solvent was then removed by cannula and the resulting solid dried in vacuo for 24 h; yield 0.036 g (70%). Anal. Calcd for $C_{18}H_{21}I_2N_2ORh$: C, 33.88; H, 3.32; N, 4.39. Found: C, 33.74; H, 3.34; N, 4.38. IR (CH_2Cl_2; ν(CO)/cm^{-1}): 2076. ^{1}H NMR (CD_2Cl_2; δ): 10.21−10.25 (bm, 1H), 8.39−7.26 (7H) (arom) 3.66 (major), 2.67 (minor) (each sept, 7 Hz, total 1H, MeC*H*Me, two conformers/isomers, ratio ca. 3:1), 2.37 (major), 2.33 (minor) (each s, total 3H, *Me*C═N), 1.33, 1.13 (major), 1.25, 1.20 (minor) (each d, 7 Hz, total 6H, *Me*CH*Me*), 1.70 (major), 1.60 (minor) (each d, $^2J_{Rh-H}$ = 2.1 Hz, total 3H, *Me*Rh).

(f) [Rh(CO)(ArN═C(Me)-2-py)I$_2$Me] (2f; Ar = 2,6-^{i}Pr$_2$C$_6$H$_3$). In an in situ NMR experiment, [Rh(CO)(ArN═C(Me)-2-py)I] (**1f**; Ar = 2,6-^{i}Pr$_2$C$_6$H$_3$; 16 mg) was dissolved in CD_2Cl_2 (0.7 cm^3) in an NMR tube, to which was added methyl iodide (10-fold excess/**1f**) at room temperature. The initial ^{1}H NMR spectrum revealed doublets at δ 1.77, 1.58, and 1.49 (each with $^2J_{Rh-H}$ = 2.1 Hz) in the ratio ca. 5:5:1 assigned to methyl ligands of isomers of **2f**. A singlet at δ 3.30 is assigned to the acetyl product **3f** in equilibrium with the methyl species. Integration of the signals indicates a methyl to acetyl ratio of ca. 1:3 at equilibrium. A characteristic signal at δ 10.24 (m) is assigned to the hydrogen at position 6 on the pyridyl ring of **3f**. IR (CH_2Cl_2; ν(CO)/cm^{-1}): 2073 (**2f**) 1716 (**3f**).

(g) [Rh(CO)(2,2′-bipy)I$_2$Me] (2g). [Rh(CO)(2,2′-bipy)I] (**1g**; 16 mg) was dissolved in CD_2Cl_2 (0.7 cm^3) in an NMR tube, to which was added methyl iodide (10-fold excess/**1g**) at room temperature. The initial ^{1}H NMR spectrum revealed doublets

Table 3. Summary of Crystallographic Data for Complexes 1f, 2a, 3c, and 4f

	1f·CH_2Cl_2	**2a**·$CHCl_3$	**3c**·CH_2Cl_2	**4f**
formula	$C_{21}H_{26}Cl_2IN_2ORh$	$C_{25}H_{32}Cl_3I_2N_2ORh$	$C_{31}H_{45}Cl_2I_2N_2ORh$	$C_{20}H_{24}I_3N_2ORh$
fw	623.15	839.59	889.30	792.02
cryst syst	orthorhombic	orthorhombic	orthorhombic	monoclinic
space group	*Pbca*	$Pna2_1$	*Pnma*	$P2_1/c$
color	black	red	brown	black
a (Å)	16.0948(11)	15.4058(9)	18.249(4)	10.793(4)
b (Å)	14.5096(10)	10.6809(6)	18.634(4)	13.266(4)
c (Å)	20.7994(15)	18.1516(11)	10.630(2)	16.881(5)
α (deg)	90	90	90	90
β (deg)	90	90	90	100.524(7)
γ (deg)	90	90	90	90
temp (K)	150(2)	150(2)	293(2)	150(2)
Z	8	4	4	4
Flack param		0.28(9)		
final *R* indices ($I > 2\sigma(I)$)				
R1	0.0338	0.0573	0.0555	0.0502
wR2	0.0653	0.1498	0.1351	0.0874
R indices (all data)				
R1	0.0677	0.0737	0.0758	0.1427
wR2	0.0737	0.1610	0.1478	0.1097
GOF	0.922	1.038	1.052	0.827

at δ 1.41 ($^2J_{Rh-H} = 2.1$ Hz) and δ 1.96 ($^2J_{Rh-H} = 1.8$ Hz) in the ratio ca. 20:1 assigned to methyl ligands of isomers of **2g**. A characteristic signal at δ 10.18 (m) is assigned to the hydrogen at position 6 on a pyridyl ring of **2g**. On prolonged reaction (17 h) a weak singlet was observed at δ 3.46 corresponding to a small amount of the acetyl product **3g**. The doublet at δ 1.96 had grown relative to that at δ 1.41, indicating slow isomerization of **2g**. IR (CH_2Cl_2; ν(CO)/cm^{-1}): 2071 (**2g**).

(h) [Rh(CO)(ArN═C(Me)-2-py)I$_3$] (4f; Ar = 2,6-^{i}Pr$_2$C$_6$H$_3$). [Rh(CO)(ArN═C(Me)-2-py)I] (**1f**; 0.030 g, 0.06 mmol) was dissolved in THF (10 cm^3) under N_2. On addition of iodine (0.014 g, 0.06 mmol of I_2) the solution rapidly changed color from dark purple to brown. After the mixture was stirred for 30 min, the solvent was removed in vacuo and the resulting black solid was recrystallized by dissolution in THF (2.5 cm^3) and dropwise addition of pentane (25 cm^3) to precipitate the product; yield 33 mg (76%). Anal. Calcd for $C_{20}H_{24}I_3N_2ORh$: C, 30.3; H, 3.1; N, 3.5. Found: C, 31.0; H, 3.1; N, 3.3. IR (CH_2Cl_2; ν(CO)/cm^{-1}): 2092. ^{1}H NMR (CD_2Cl_2; δ): 10.27 (m, 1H), 8.26 (m, 1H), 8.17 (m, 1H), 7.85 (m, 1H), 7.45−7.35 (bm, 3H) (arom), 3.60 (m, 2H, Me_2CH), 2.55 (s, 3H, C(*Me*)═N), 1.36, 1.05 (each d, 7 Hz, 6H, Me_2CH). A single crystal of **4f** suitable for X-ray diffraction (vide infra) was obtained by recrystallization from dichloromethane.

X-ray Structure Determinations. Data were collected on either a Bruker Smart CCD area detector with Oxford Cryostream 600 low-temperature system (complexes **1f**, **2a**, and **4f**) or a Siemens P4 diffractometer (complex **3c**), in each case using Mo Kα radiation ($\bar{\lambda} = 0.710\ 73$ Å). The structures were solved by direct methods and refined by full-matrix least-squares methods on F^2. Hydrogen atoms were placed geometrically and refined using a riding model (including torsional freedom for methyl groups). Complex scattering factors were taken from the SHELXTL program package.[34] Crystallographic data are summarized in Table 3, and full listings of data are given in the Supporting Information.

Kinetic Experiments. Samples for kinetic runs were prepared by placing the required amount of freshly distilled methyl iodide in a 5 cm^3 graduated flask which was then made up to the mark with the solvent of choice (usually CH_2Cl_2). A portion of this solution was used to record a background spectrum. Another portion (typically 500 μL) was added to the solid metal complex (typically 7−8 μmol) in a sample vial to give a reaction solution with a complex concentration of ca. 15 mM. A portion of the reaction solution was quickly transferred to the IR cell, and the kinetic experiment was started. To obtain pseudo-first-order conditions, at least a 10-fold excess of MeI was used, relative to the metal complex. The IR cell (0.5 mm path length, CaF_2 windows) was maintained at constant temperature throughout the kinetic run by a thermostated jacket. Spectra were scanned in the metal carbonyl ν(CO) region (2200−1600 cm^{-1}) and saved at regular time intervals under computer control. After the kinetic run, absorbance vs time data for the appropriate ν(CO) frequencies were extracted and analyzed off-line using Kaleidagraph curve-fitting software. The decays of the bands of **1a**−**e**,**g** were all well fitted by exponential curves with correlation coefficients ≥0.999, to give pseudo-first-order rate constants. Each kinetic run was repeated at least twice to check reproducibility, the k_{obs} values given being averaged values with component measurements deviating from each other by ≤5%. For the reaction of **1f** with MeI, the absorbance vs time data for bands of **1f**, **2f**, and **3f** were fitted to a two-step reversible kinetic model (Scheme 2) using a Microsoft Excel spreadsheet.

Acknowledgment. This work was supported by BP Chemicals Ltd. (studentships to L.G. and J.A.G.), the EPSRC, and the University of Sheffield.

Supporting Information Available: Tables of kinetic data and figures giving ORTEP plots; crystallographic data are also available in CIF format. This material is available free of charge via the Internet at http://pubs.acs.org.

OM020777W

(34) Sheldrick, G. M. SHELXTL, An Integrated System for Solving and Refining Crystal Structures from Diffraction Data (Revision 5.1); Bruker AXS Ltd., Madison, WI.